Research Article

NEWLY ANTIBACTERIAL / ANTI-RUSTING OXADIAZOLE-PYROMELLITIC DIIMIDE OF CARBON STEEL /HYDROCHLORIC ACID INTERFACE: TEMKIN ISOTHERM MODEL

Ahlam Marouf Al-Azzawi[1*] and Kafa Khalaf Hammud[2]

[1]Department of Chemistry, College of Science,
University of Baghdad, Baghdad, Iraq.
[2]Ministry of Science & Technology, Baghdad, Iraq.

ABSTRACT

In this work, new pyromellitic diimide linked to oxadiazole cycle was synthesized via multistep processing. In the first step, pyromellitic diimide (1) was prepared by the reaction of its dianhydride with urea by conventional and under microwave irradiation method. Treatment of compound (1) with alcoholic KOH in the second step afforded the corresponding potassium salt (2). Compound (2) was introduced in reaction with ethyl chloroacetate in the third step producing compound (3) ethyl-2- (N-pyromellitic diimidyl) acetate. In the fourth step, compound (3) on treatment with hydrazine hydrate afforded the corresponding acetohydrazide (4) and this in turn was subjected to the fifth step in reaction with carbon disulfide in alcoholic KOH solution producing the target compound (5). Corrosion inhibition efficiency of 50 ppm compound (5) was studied in 0.3 N HCl at different temperatures. Also, antifungal and antibacterial activities of compound (5) was evaluated with different microbial species and showed a good inhibition against all tested microorganisms.

The main goal of this research was directed to study the adsorption mechanism of this good antibacterial oxadiazole –pyromellitic diimide (5) with carbon steel in acidic medium (0.3N HCl). Calculated equilibrium constant ($K_{ads.}$) values were increased with temperature raise reflecting the excellent efficiency of adsorption at the studied conditions as a good antibacterial corrosion inhibition derivative.

Keywords: pyromellitic diimide, corrosion, oxadiazole, acetohydrazide, Temkin model.

INTRODUCTION

Metal corrosion is a serious industrial problem all over the world. One of the most effective protections is using inhibitor especially organic with oxygen, nitrogen, or sulfur as electronegative atom beside aromatic ring or triple bond that afforded electronic cloud. These different organic inhibitors are working depending on two basic considerations. The first is availability of N, O, S, CN, C≡C, aromatic ring…etc. as previously mentioned that enhanced adsorption while the second basic consideration is the economic-environmental concept of these materials [1-5].

1,3,4- Oxadiazoles are important member in heterocyclic family with known applications in biological, photosensitive, electrical, and corrosion materials [6-9]. Also, cyclic imide is important moiety in organic chemistry which were successfully applied as a biological, pharmaceutical, corrosion inhibitor, fluorescent dye, chemosensor optically induced anisotropy, and other applications [10].

For all above mentioned reasons, we planned and achieved a new organic design of synthesis with two applications (antimicrobial and corrosion inhibitory). The organic design was featured with dicyclic imide moiety with di (1,3,4-oxadiazole) presence. The last planned step was studying the adsorption mechanism of this dicyclic imide – oxadiazole derivative with Temkin isothermal model.

Experimental section
Instruments
Domestic microwave oven, SHOWNIC, China was used for organic section. Melting points were determined on Gallenkamp capillary melting point apparatus. FTIR spectra were recorded using KBr discs on Shimadzu FTIR-8400 Fourier Transform Infrared spectrophotometer in Ministry of Science and Technology and in Ibn Sina General Company, Ministry of Industry and Minerals. ^{1}H-NMR and ^{13}C-NMR spectra were recorded on near magnetic resonance Bruker, Ultrashield 300 MHz in Jordan, using tetramethylsilane as internal standard and deuterated dimethyl sulfoxide (DMSO-d_6) as solvent. SpectroMax$_x$, stationary metal analyser, AMETEK Spectro-Analytical Instrument (Germany, 2012 / model), in State Company for Inspection and engineering Rehabilitation (S.L.E.R), Ministry of Industry and Minerals was applied for elemental analysis of carbon steel specimen.

CHEMICALS
All used chemical were from trusted company (Fluka, BDH, and Merck) and used without further purification.

Preparation of pyromellitic diimide (1)
Conventional method[11]
Pyromellitic anhydride (0.02 mol, 4.36 g), urea (0.05 mol, 3g) were mixed, homogenized in a flask, and heated in an oil bath. When reaching (230-240) °C, the mixture began melting, and then was slowly brought to 260°C until it completely turned into liquid. Immediately, a mass of yellow crystals appeared and swelled to as 3-4 times as the initial. The crystals were cooled and dispersed by adding water (250 mL), recrystallized with water repeatedly, filtered, and dried. Yield (75%), m.p. (> 320°C).

Microwave irradiation method[12]
Reaction between pyromellitic anhydride (0.02 mol, 4.36 g) and urea (0.05 mol, 3g) in domestic microwave oven for ten minutes with 90% power gave recrystallized white crystals from water. Yield (92%), m.p. (> 320°C).
FTIR (cm^{-1}): 3448 and 3197 [v(N-H) imide], 1770 [asym. v(C=O) imide], 1716 and 1693 [sym. v(C=O) imide], 1566 cm^{-1} [v(C=C) aromatic.
Compound (1) was converted to its potassium salt (2) via its treatment with alcoholic potassium hydroxide in order to increase the nucleophilicity of nitrogen atom for attacking electron-deficient carbon in next synthesis step.

Preparation of pyromellitic diimide Potassium Salt (2)
Pyromellitic diimide (0.01 mol) was dissolved in (5 mL) of N,N-dimethyl formamide then the clear solution was added to alcoholic potassium hydroxide solution [(0.01 mol) in (25 mL) of absolute ethanol] with stirring. The obtained precipitate was filtered and dried[13].

Synthesis of ethyl-2-(N-(pyromellitic diimidyl)) acetate (3)
Potassium salt (2) (1g) and (10 mL) of pure dimethyl sulfoxide were thoroughly mixed, (5 mL) of ethyl chloroacetate was added, and the mixture was heated for one hour under a reflux condenser. After cooling, (10 mL) water was added and the product was collected by filtration, dried, and recrystallized from glacial acetic acid[13].
FTIR (cm^{-1}): 1774 [v(C=O) ester], 1720 [v(C=O) imide], 1392 [v(C-N) imide], (1215 and 1118)[v(C-O) ester]. ^{1}HNMR (δ, ppm): 1.2 [triplet, (CH$_3$) protons], (4.2-4.4) [quartet, (-OCH$_2$CH$_3$) protons], 4.5ppm [(-N-CH$_2$-CO-) protons], 8.3ppm [aromatic protons]. ^{13}CNMR (δ, ppm): 13.9[CH$_3$], 48.4 [-OCH$_2$-], 61.5 [-N-CH$_2$-], 118.1-137.2 [aromatic carbons, 165.5 [C=O) imide], 167.1-168.4 [(C=O) ester] carbons.
Compound (3) derived from the main synthone (1) via treatment of the prepared potassium salt (2) with ethyl chloroacetate under reflux condition and gave positive results in characteristic test for esters. The reaction here was performed via nucleophilic attack of negative nitrogen in pyromellitic imide moiety on electron-deficient carbon in ethyl chloroacetate.
The third step involved the conversion of the prepared ester (3) to the corresponding acetohydrazide (4) with hydrazine hydrate under reflux for ten hours as nucleophilic substitution reaction including the attack of the strong nucleophile (-NH$_2$ hydrazine) on carbonyl group.

Synthesis of 2-(N-(pyromellitic diimidyl))acetohydrazide (4)
A solution of the prepared ester [59] (0.01mol, 3.88g) in ethanol (150 mL) was mixed with hydrazine hydrate (98%, 0.02 mol, 1g, 1mL). The reaction mixture was refluxed for ten hours then was added to ice-water with stirring and left to stand for 10 hrs. The resulted product was filtered and washed with water then with petroleum ether [14]. FTIR (cm^{-1}): disappearance of absorption bands [v(C=O) and v(C-O) ester] and appearance of absorption bands (3321 and 3267) [v(NH-NH$_2$)], and (1666, 1639, 1566, and 1377) cm^{-1}

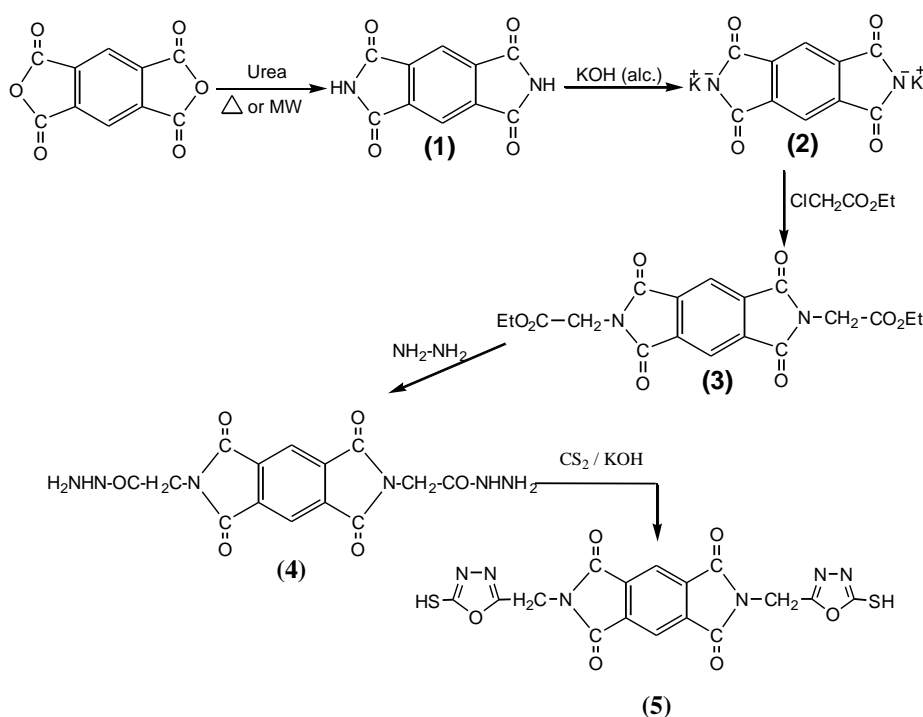[ν(C=O) imide, ν(C=O) amide, ν(C=C) aromatic, and ν(C-N) imide respectively].

Synthesis of N,N'- bis [methylene(meracpto-1,3,4-oxadiazole-2-yl)] Pyromellitic diimide (5)[15]

Acetohydrazide (4) (0.002 mol, 0.72 g) was dissolved in a solution of potassium hydroxide (0.004 mol, 0.22 g) in ethanol (20 mL). Carbon disulfide (2 mL) was then added while stirring and the reaction mixture was heated under reflux for twenty hours. The solvent was removed from the deep red solution under reduced pressure then the residue was treated with water and then filtered. The filtrate was cooled, neutralized to pH 6 using dilute hydrochloric acid and the separated product was filtered, washed with water, and dried. Recrystallization of the product from ethanol afforded the target compound (5). FTIR (cm^{-1}): 3460 [ν(NH) formed due to tautomerism], 1700, 1639, 1593, and 1365 [ν(C=O) imide, ν(C=N), ν(C=C) aromatic, and ν(C-N) imide respectively], 1273 and 1184 [ν(C-O-C) oxadiazole], and 655 [ν(C-S)]. ^{1}HNMR (δ, ppm): 5.27 [(-CH$_2$-) protons], 7.15 [aromatic protons], and 8.6 ppm [NH and SH protons]. ^{13}CNMR (δ , ppm): 72.8 [(-CH$_2$-) carbons], 123.2-129.1 [aromatic carbons], and (153.9 and 181.4) ppm [(C=N) and (C=O) carbons respectively].

Synthesis of the target compound (5) was performed by multistep procedure which are summarized in scheme -1-.

Scheme -1-

Biological activity

Compounds (1, 3, and 5) were tested for their in vitro growth inhibitory activity against *Staphylococcus aureus*, *Escherichia coli*, *Pseudomonas aeruginosa*, and *Bacillus subtilis* bacteria and against *Candida albicans* fungi by applying cup plate method using nutrient agar medium and dimethyl sulfoxide that used as a sample solution [16].

The test organisms were first cultured in nutrient broth and incubated for 24 hours at 37°C and then freshly prepared bacterial cells were spread onto the Nutrient Agar while fungal spores onto Potato Dextrose Agar in laminar flow cabinet. The tested compounds were previously dissolved in dimethyl sulfoxide then (0.1 mL) of each compound (known concentration) was added in the cups and the Petri dishes were subsequently incubated at 37°C for 24 and 48 hrs. Inhibition zone produced by each compound was measured in (mm).

In our present work, compounds (1, 3, and 5) were tested for their in vitro growth inhibitory activity against *Staphylococcus aureus*, *Escherichia coli*, *Pseudomonas aeruginosa*, *Bacillus subtilis* , and *Candida albicans* by applying cup-plate agar diffusion method and the inhibition zones were measured (Table 1). The results showed that compound (5) was highly or very highly active on the all tested species.

Table 1: Biological activities against different microorganisms

Comp. No.	*Staphylococcus aureus* Conc., mg/ mL (DMSO)	Inhibition zone, mm 24 hrs	Inhibition zone, mm 48 hrs	*Bacillus subtilus* Conc., mg/ mL (DMSO)	Inhibition zone, mm 24 hrs	Inhibition zone, mm 48 hrs	*Escherichia coli* Conc., mg/ mL (DMSO)	Inhibition zone, mm 24 hrs	Inhibition zone, mm 48 hrs	*Pseudomonas aeruginosa* Conc., mg/ mL (DMSO)	Inhibition zone, mm 24 hrs	Inhibition zone, mm 48 hrs	*Candida albicans* Conc., mg/ mL (DMSO)	Inhibition zone, mm 24 hrs	Inhibition zone, mm 48 hrs
1	5.0	12		5.0	-ve		5.0	12		5.0	9		5.0	10	
	10.0	12		10.0	-ve		10.0	11		10.0	7		10.0	9	
	20.0	13		20.0	-ve		20.0	13		20.0	9		20.0	-ve	
3	5.0	-		5.0	-ve		5.0	-ve		5.0	-		5.0	5	
	10.0	-		10.0	20		10.0	-ve		10.0	-		10.0	20	
	20.0	-		20.0	5		20.0	-ve		20.0	-		20.0	-ve	
5	5.0	13		5.0	7		5.0	-ve		5.0	-ve		5.0	10	
	10.0	14		10.0	10		10.0	14		10.0	13		10.0	15	
	20.0	18		20.0	12		20.0	17		20.0	15		20.0	17	

Corrosion study

Instruments used in this work are Corrosion call and electrode, HAAKE 000-3959, Germany, Electric balance, FR-180 A, A & D, Magnetic stirrer, 400, China, Potentio- state Mlab 2000, Germany, Thermocouple, USA, and Chiller, HAAKE 000-3959, Germany.

Specimen Characterization

The material composition employed for the present work was characterized with SpectroMax$_x$/ stationary metal analyser) to specify its actual metallurgical type (in percent) which were C:0.187 , Si: 0.311, Mn:1.03 , P:0.007, S: 0.012, Cr: 0.003, Mo: 0.002, Ni: 0.029, Al: 0.038, Co: 0.001, Cu: 0.002, W: 0.222, As: 0.0083, Fe, 98.3 beside V, Pb, Sn, Zr, Bi, Ca, Ce, B, Zn, and La in trace amounts.

Sample preparation

The investigated material was carbon steel which fabricated in circular samples with dimensions of 2.5 cm in diameter. The experimental procedure was based on the standard reference method for making potentiostatic polarization measurement and was under the jurisdiction of ASTM committee G1 on corrosion of metals.

Corrosion cell made of Pyrex with (1L) capacity consists of two vessels, internal and external. Chiller device was used to make the temperature of water which flows through the external vessel constant at 25^oC. Three electrodes and thermostat was replaced in the internal vessel. Reference Electrodes here is used to determine the working electrode potential according to the potential of reference electrode. The potential of reference electrode is well known and accurate, and it is combined of two tubes; the inner tube contains mercury, mercurous chloride, and chloride ion. The outer tube filled with the prepared acidic solution (with or without inhibitor).

The calomel electrode could be prepared by grinding calomel (Hg_2Cl_2), mercury and a small quantity of saturated KCl solution together and placing the resultant slurry in a layer about (1 cm) thick on the surface of mercury contained in a clean test tube. External contact to the mercury was usually made by a platinum wire, which was sealed, to glass.

The reference electrode replaced at the distance two mm from working electrode which is usually brought in contact with the electrolyte through a glass tubing as "Luggin capillary" which is filled by the test solution. The tip of the Luggin capillary is placed in the electrochemical cell very close to the working electrode.

Such arrangement allowed the calomel electrode to be removed entirely from the class Luggin envelope to replenish the bridge solution whenever need and eliminated any drop that may develop in the solution separating the calomel electrode and the working electrode in the cell solution.

The auxiliary electrode consists of high purity platinum metal; its length is (10 cm). The working electrode is the studying and testing subject which potential will be measured; this electrode is formed from 20 cm length metallic wire and connected to the mounted specimen.

The specimen subjected in the holder in which the diameter of the exposed surface to the solution is (1 cm^2). To determine the open circuit potential of the specimens, the specimens have been immersed in the acidic solution prepared in the laboratory to reach the steady state between the specimen's material and electrolytic solution. The change in potential according to the current was determined during (5 min), and time step equal to 60 sec. for each specimens. After reaching the steady state condition, the determined potential is known as corrosion potential or free potential or open circuit potential.

In the base of the Tafel extrapolation, under the theorem of mixed potentials, is considered to determine the corrosion rate and values of potential from cathodic and anodic polarization. After determining the open circuit potential, low current from cathodic current

was passed through the specimens by reducing magnitude of variable resistance gradually. Then the working electrode potential was measured against the current. By potentiostat device, a final result (value of current density) was analyzed as current-potential data with using potentiostat device software (Tables 2-5, Figure 1).

Table 2: Values of the open circuit potential (OCP), the corrosion potential (E$_{corr}$), the corrosion current densities (I$_{corr}$), weight loss (wt loss), penetration loss, protection efficiency (P%), and Surface Coverage (θ) for carbon steel in (0.3N) hydrochloric acid with compound (5) at four different temperatures

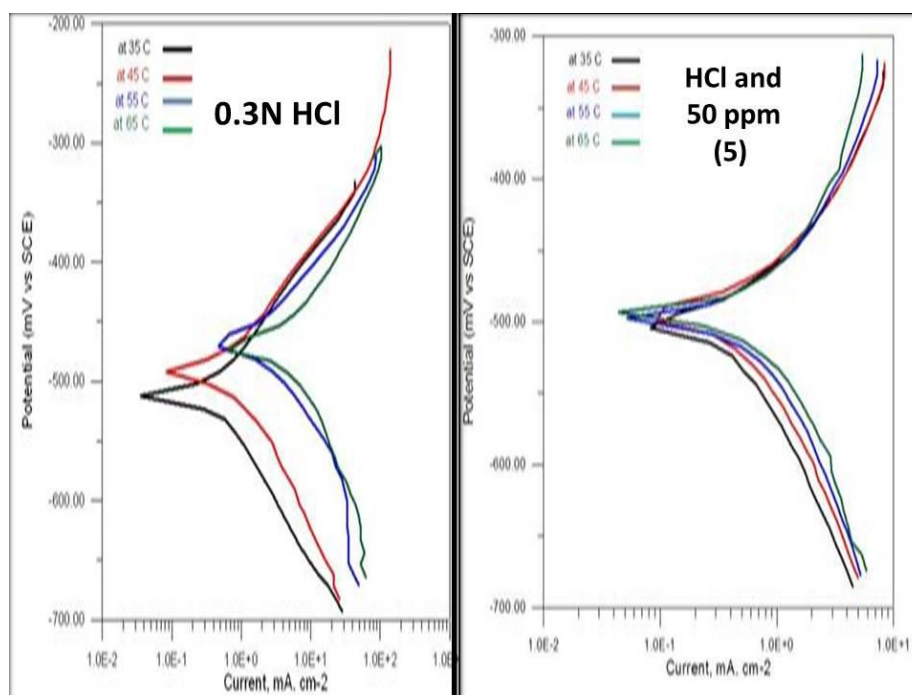| Condition	Conc.	Temp., K	OCP, V	E$_{corr}$, V	I$_{corr}$, A/ cm^{-2} (x10^{-6})	Wt loss, g.m^{-2}.d^{-1}	Penetration, mm. y	P%	θ
HCl	0.3N	308	-0.513	-0.5114	383.83	96.00	4.46	-	-
		318	-0.503	-0.4916	515.86	129.00	5.99	-	-
		328	-0.492	-0.4709	1310.00	329.00	15.30	-	-
		338	-0.484	-0.4735	3450.00	862.00	40.00	-	-
5	50 ppm	308	-0.505	-0.5044	302.78	75.70	3.51	21.1458	0.2114
		318	-0.500	-0.4984	345.15	86.30	4.01	33.1007	0.3310
		328	-0.498	-0.4968	488.87	122.00	5.67	62.9179	0.6291
		338	-0.494	-0.4923	522.02	130.00	6.06	84.9187	0.8491

Fig. 1: The polarization curve of carbon steel in 0.3N HCl and different concentration of compound (5) at different temperatures.

Table 3: Values of the Tafel slopes ($\square_a$, $\square_c$), transfer coefficients (α_a, α_b), polarization resistance (Rp), and equilibrium exchange current density for polarization carbon steel in (0.3N) hydrochloric acid with compound (5) at four different temperatures

Condition	Conc	Temp., K	I_{corr}, A/ cm^{-2} ($\times 10^{-6}$)	$\square_a$, V.decade^{-1}	$\square_c$, V. decade^{-1}	α_a	α_b	Rp, Ω.cm^{-2} ($\times 10^4$)	I_o, A/ cm^{-2} ($\times 10^{-6}$)
HCl only	0.3 N	308	383.83	-0.0945	0.0859	0.6467	0.7115	0.1332	19.9195
		318	515.86	-0.0847	0.0817	0.7450	0.7724	0.0952	28.7539
		328	1310.00	-0.0681	0.0749	0.9558	0.8690	0.0359	78.6260
		338	3450.00	-0.0936	0.0973	0.7166	0.6893	0.0137	212.2101
5	50 ppm	308	302.78	-0.1207	0.0872	0.4669	0.7009	0.1665	15.9313
		318	345.15	-0.1203	0.0895	0.4843	0.7050	0.1444	18.9761
		328	488.87	-0.1412	0.1051	0.4567	0.6193	0.1016	27.8122
		338	522.02	-0.1322	0.1086	0.5100	0.6176	0.0943	30.8833

Table 4: The thermodynamic quantities carbon steel in sulfuric acid at different concentration of compound (5) at four different temperatures

Condition	Conc.	Temp., K	OCP, V	E_{corr}, V	-ΔG, KJ/mol	ΔS, KJ/mol. K	ΔH, KJ/mol
HCl	0.3 N	308	-0.513	-0.5114	98.68486		18.91286
		318	-0.503	-0.4916	94.86405	0.259	12.50205
		328	-0.492	-0.4709	90.86957		5.917573
		338	-0.484	-0.4735	91.3713		3.829295
5	50 ppm	308	-0.505	-0.5044	97.33407		74.85007
		318	-0.500	-0.4984	96.17625	0.073	72.96225
		328	-0.498	-0.4968	95.8675		71.9235
		338	-0.494	-0.4923	94.99913		70.32513

Table 5: Kinetic quantities for carbon steel in (0.3N) hydrochloric acid with different concentrations of compound (5) at four different temperatures

Condition	Conc.	Temp., K	I_{corr}, A/ cm^{-2} ($\times 10^{-6}$)	E_a, KJ/mol.	A, Molecules/ cm^2.s	ΔS^*, KJ/mol. K	ΔH^*, KJ/mol.
HCl only	0.3 N	308	383.83	64.6790	7.1167 x 10^{15}	0.3866	61.9984
		318	515.86				
		328	1310.00				
		338	3450.00				
		318	487.39				
		328	1090.00				
		338	2540.00				
5	50 ppm	308	302.78	17.1807	1.5285 x 10^{18}	0.2321	14.5001
		318	345.15				
		328	488.87				
		338	522.02				

RESULTS AND DISCUSSION

The present work aimed to synthesize new compound that can be act as a corrosion inhibitor for carbon steel in acidic medium.

Chemical structure of the newly synthesized target compound (5) N,N'- bis [methylene(meracpto-1,3,4-oxadiazole-2-yl)] Pyromellitic diimide or that may be named as 2-(N-(pyromellitic diimidyl))-1,3,4-Oxadiazole-5-Thiol contains all the important electronegative heteroatoms including oxygen, nitrogen, and sulfur which are presented in oxadiazole ring substituted with thiol group. π electron cloud is also presented in the aromatic system in pyromellititc diimide component which contains two nitrogen heterocycle fused with benzene ring.

A convenient way to express the corrosion behaviour of a metal is by considering its potential–current density diagram which is generally known as the polarization curve (Figure 1). The corrosion potential (E_{corr}) of a material in a certain medium at a constant temperature is a thermodynamic parameter in which under the equilibrium potential (in opposite sign) of the cell consisting of the working electrode and the auxiliary electrode, the rate of anodic dissolution of working electrode material becomes equal to the rate of the cathodic process that takes place on the same electrode surface.

When (E_{corr}) becomes more negative, the potential of the Galvanic cell becomes more positive and the Gibbs free energy change (ΔG) for the corrosion process becomes more

negative. The corrosion reaction is then expected to be more spontaneous on pure thermodynamic ground.

When the measured value of (E_{corr}) becomes less negative, the potential of the corresponding Galvanic cell becomes less positive, hence the (ΔG) value for the corrosion process becomes less negative, and the process is thus less spontaneous.

The corrosion current density (i_{corr}) is a kinetic parameter and represents the rate of corrosion under specified equilibrium condition. The obtained data indicate that (i_{corr}) can be summarized as below (Table 2)

- i_{corr} value for carbon steel in the applied acidic media without inhibitor is higher than with applied inhibitor which referred to its efficiency in general view.
- i_{corr} values increased with temperature and acid concentration increasing.

Generally, the protection efficiency (P%), which was calculated from weight loss (g/m^2.d) data not from i_{corr}, was decreased with temperature increasing and may be affected with acid concentration, acid composition, and chemical structure of the tested inhibitor (Table 2).

Organic compounds are adsorbed on the metal surface and interface with either cathodic or anodic reaction occurring at the adsorption site. From deep analysis of the polarization curves which have been obtained for at four temperatures, it was possible to derive data concerning (the cathodic (β_c) and anodic (β_a) Tafel slopes) and (the cathodic (α_c) and anodic (α_a) transfer coefficients).

Values of α have been calculated from the corresponding values of the Tafel slope (β) using the relation [17]:

α_c= 2.303RT/ β_c F   and α_a= 2.303RT/ β_a F

where R is the gas constant and F is the Faraday constant.

A value of the cathodic transfer coefficient α_c of $\simeq$ 0.5, or of the cathodic Tafel slope of (-0.12 V.decade^{-1}), may be diagnostic of a proton discharge–chemical desorption mechanism in which the proton discharge is the rate–determining step.

If the chemical desorption is the rate – determining step, the rate would be independent of the overpotential since no charge transfer occurs in such a step and the rate becomes directly proportional to the concentration or the coverage (θ) of adsorbed hydrogen atoms [18]. On the other hand, if the discharge process is followed by a rate – determining step involving chemical desorption, the expected value of α should be (2.0).

The obtained results indicated that the variation of the Tafel slopes and of the corresponding transfer coefficients could be interpreted in terms of the variation in the nature of the rate–determining step from charge transfer process to either chemical–desorption or to electrochemical desorption.

The obtained values of the (cathodic (β_c) and anodic (β_a) Tafel slopes) and (the cathodic (α_c) and anodic (α_a) transfer coefficients) were differed after the newly synthesized heterocyclic derivatives that indicated to their effects on the metal dissolution and subsequently the corrosion process at all.

The polarization resistance, R_p, according electrode, is defined as the slope of a potential (E)–current density (i) plot of the corrosion potential (E_{corr}) as:

$$R_p = \left(\frac{\partial \eta}{\partial i} \right)_{T,C} at\, \eta \to 0$$

Where $\eta = E - E_{corr}$, is the extent of polarization of the corrosion potential and (i) is the current density corresponding to a particular value of (η). From the polarization resistance R_p, the corrosion current density i_{corr} can be calculated as :

$$i_{corr} = \beta / R_p$$

Where β is a combination of the anodic and cathodic Tafel slopes (β_a, β_c) as:

$$\beta = \beta_a \beta_c / 2.303 (\beta_a + \beta_c)$$

For the general case, by inserting (β) from the previous equation in ($i_{corr} = \beta / R_p$) equation one obtains the so–called the Stern – Geary equation [19]:

$$R_p = \beta_a \beta_c / (2.303 (\beta_a + \beta_c) i_{corr})$$

The measurement of polarization resistance has very similar requirements to the measurement of full polarization curves and it is particularly useful as a method to rapidly identifying corrosion up-setting and initiating remedial action [20].

The term (E_{corr} /i_{corr}) corresponds to the resistance (R) of the metal/solution interface to charge–transfer reaction. It is also a measure of the resistance of the metal to corrosion in the solution in which the metal is immersed. The reaction resistance (R_p), which mainly depends upon the equilibrium exchange current density (i_o) determines what may be termed the polarizability, i.e., what overpotential ($\eta = E - E_{corr}$) a particular current density needs (for a driven cell) or produces (for a spontaneously performing cell).

The results of the polarization resistance (R_p) (calculated from term (E_{corr} /i_{corr}) for the corrosion of carbon steel in different acidic media with different inhibitors at four different temperatures can be summarized as follow (Table 3):

1.   For all applied condition, R_p decreased with temperature range increasing.

2.   The decreased of R_p values imply increasing corrosion rate and vice versa.

The free-energy change accompanying an electrochemical reaction can be calculated by the following equation [21]

$$\Delta G = -nFE$$

where *ΔG* is the free-energy change, *n* is the number of electrons involved in the reaction, *F* is the Faraday constant, and *E* equals the cell potential ($E = E_{corr}$).

From the value of *ΔG* at several temperatures, the change in the entropy (*ΔS*) of corrosion process could be derived according to the well-known thermodynamic relation:

$$\Delta S = -d(\Delta G) / dT$$

Values of *ΔG* are usually plotted against temperature (T); thus at any temperature the value of [s – *d(ΔG)/dT= ΔS*] which corresponds to the slope of the *(- ΔG)* versus (T) plot at that temperature.

The change in free energy, ΔG, is related to ΔH, the change in the enthalpy, and ΔS, the change in entropy of the corrosion reaction at a constant temperature, T, by the equation [21]:

$$\Delta G = \Delta H - T \Delta S$$

When a metal undergoes corrosion, there is a change in Gibbs free energy (ΔG) of the system, which is equal to the work, associated with the corrosion reaction.

The performance of such a work is accompanied usually by a decrease in the Gibbs free energy of system. The variation of the (−ΔG) for corrosion of carbon steel in the research conditions, generally values of ΔG were negative suggesting the existence of thermodynamic feasibility for the corrosion of the electrodes materials in the absence or the presence of the applied inhibitors in the acidic media (Table 4).

Values of (ΔS) were positive or negative depending on the positive or negative dependencies of (ΔG) values on temperatures. Values of (ΔS) reflect the change in the order and orientation of the solvent molecules around the hydrated metal ions in the corrosion medium when metal atoms were corroded and subsequently hydrated in the solution.

Values of ΔS were generally positive due to negativity of ΔG, this suggests a lower order in the solvated states of the metal ions as compared with the state of metal atoms in the crystal lattice of the corroding electrodes. The obtained results indicate the variation of (ΔS (KJ/mol. K)) with the absence and presence of the applied inhibitors.

Values of the enthalpy of corrosion (ΔH) reflect the enthalpy changes associated with the corrosion reaction and may be ranged from negative to positive values, according to the experimental conditions, indicating exothermic or endothermic nature of corrosion reaction. Generally, the direction of ΔH variation sequence is opposite to ΔG variation.

The rate (r) of corrosion in a given environment is directly proportional with its corrosion current density (i_{corr}) in accordance with the relation [21]:

$$r = 0.13 \, (e / \rho) \, i_{corr}$$

where (*e*) is the equivalent weight of the metal and (*ρ*) is its density. For the increasing values of (i_{corr}) with a temperature follow Arrhenius equation [22], it is reasonable as:

$$\log (i_{corr}) = -E_a / 2.303 \, RT + \log A$$

where *A* and E_a are the pre- exponential factor and energy of activation of the corrosion process respectively.

Values of E_a were derived from the slopes of the ($\log i_{corr}$) versus (1/T) linear plots while those of (A) were obtained from the intercepts of the plots at (1/T=zero); values of (A), expressed in term of (Amper. cm^{-2}), have then been converted into (molecules per cm^2 per second), (**A**) was defined as:

$$A = (KT/h) \exp (\Delta S^* / R)$$

where K, h, T, R, *ΔS** are Boltzmann constant (1.381×10^{-23} $J.K^{-1}$), Planck constant (6.62608×10^{-34} J.S), temperature on Kelvin scale, gas constant (8.314 J/Mol. K) and the entropy of activation respectively

In order to calculate the activation parameters [23] of the corrosion process, transition state equation were used with Arrhenius equation:

$$i_{corr} = (RT / Nh) \exp (\Delta S^* / R) \exp (-\Delta H^* / RT)$$

where A is the pre-exponential factor; N, h are Avogadro's number and Plank's constant respectively and E_a, ΔH^* and ΔS^* are the activation energy, change in enthalpy and change in the entropy of the corrosion

process. Straight lines are obtained with a slope of $-\Delta H^*/R$ and an intercept of $(\ln (R/Nh) + \Delta S^*/R)$ from which the values of ΔH^* and ΔS^* are calculated.

In the present study, the values of A, E_a, ΔS^*, and ΔH^* were calculated and showed (Table 5) that E_a values for inhibited solution are higher than the value for inhibitor-free solution. The increase in activation energy in the presence of inhibitors signifies physisorption [24]. However, in which the higher value of E_a for the inhibited system indicates physical adsorption in the initial stage, cannot be taken into account as decisive because of competitive inhibitor adsorption on the metal surface with water, whose desorption from the surface requires some activation energy [25].

Therefore, the adsorption phenomenon of organic inhibitor molecules on the metal surface is not considered only as physical or chemical adsorption [24].

Typically, the enthalpy of physisorption process is lower than that of 40.00 kJ/ mol while the enthalpy of chemisorptions process approaches 100kJ/mol [26].

- The positive sign of ΔH^* suggests that the dissolution process is endothermic in nature and its dissolution is slow [25]. In the presence of tested compounds, E_a and ΔH^* values change in a similar manner. These results verify the known thermodynamic relationship [27] between E_a and ΔH^*:

$$(\Delta H^* = E_a - RT)$$

- Generally, the values of ΔS^* are higher for inhibited solutions than for uninhibited solution. This might be the result of the molecular adsorption, which could be regarded as a semi-substitution process between the molecules in the aqueous phase and water molecules on the carbon steel surface [24].

The adsorption Mechanism

The molecular structure is one of the major factors influencing the adsorption of the organic molecules on the metal surface, and hence the inhibitor properties, especially in the case of chemisorption, which involves charge sharing or charge transfer from the inhibitor molecules to the metal to form coordinate type of bonds. The electronic density of the atoms, acting as reaction centers of the molecules, determines the adsorption bond.

So the influence of the chemical structure is limited to the molecular area in the adsorbed state, because it determines the area of the metal, shielded by the inhibitor.

Owing to the acidity of the medium [4, 27], the N, O, and S heteroatom could not remain in solution as free acids or bases. They exist as a neutral species or in the cationic form. Thus, the adsorption of the examined molecules could be occurred due to the formation of a links between the d-orbital of iron atoms, involving the displacement of water molecules from the metal surface, and the lonely sp^2 electron pairs present on the N, O, S atoms of the heterocyclic rings.

Moreover, these compounds may also adsorb through the electrostatic interactions between the positively charged nitrogen atom and the negatively charged metal surface. Thus, the better performance of the tested compounds in acidic solutions can be related to the specific adsorption of anions having a smaller degree of hydration, such as chloride ions, which is expected to be more pronounced. Being specifically adsorbed, they create an excess negative charge toward the solution and favor more adsorption of the cations.

In general, introduction of substituent R withdrawing electrons from the aromatic ring decreases the density of p-electrons in the ring. Consequently, the positive charge density of the cationic form is increased in which its adsorption on the negative sites of the metal surface is reinforced as a result of the increased coulombic interaction.

The high p-electron density of the heterocyclic moiety comes from the high electronegativity of its oxygen hetero-atom in addition to the presence of electron donating group which attached directly to the heterocyclic moiety. This in turn leads to decrease the positive charge density on the cationic form of the moiety, causing decrease of the inhibition effect.

The lowest inhibition efficiency [4, 27] may be a result to the absence of the positive charge. This should be attributed to the difficulty of resonance to take place in the acid medium. Moreover, the small size of compound may result in low surface coverage and consequently leading to less inhibition effect.

When the inhibitor contains carboxylic acid group, this group can react with corrosion products, which increases the protective layer thickness. This leads to slightly better corrosion inhibition.

In the uninhibited HCl solution, the mechanism of anodic dissolution involves successively the reversible adsorption of the anions (Cl^-) to the surface, release of electrons from the adsorbed anions to the metal surface and desorption of the adsorbed anions along with Fe^{2+} ions, after picking up electrons from the Fe atoms [28].

To obtain the adsorption isotherm, the linear relationship between the values of θ and the inhibitor concentration (C_{inh}) must be established. The three adsorption isotherms [29] applied to fit the surface coverage (θ) values at different concentrations of inhibitors were the Temkin isotherm:

$$K_{ads} C = e^{f\theta}$$

the Frumkin isotherm:

$$K_{ads} C = (\theta/1-\theta) e^{f\theta}$$

and the Langmuir isotherm:

$$K_{ads} C = \theta/1-\theta$$

where f (θ) is the configuration factor that depends upon the physical model and assumption underlying the derivatives of the isotherm, θ is the surface coverage, C is the inhibitor concentration, and K_{ads} is the equilibrium constant of adsorption.

In this study, the average values for free energy of adsorption (ΔG_{ads}), were calculated by using the following equation (Temkin isotherm) (Table 6):

$$K= \theta/(1- \theta) C$$
$$K= (1/55.5) \exp (\Delta G_{ads}/ RT)$$

where θ is degree of coverage on metal surface, C is concentration of inhibitors in mol/L, R is molar gas constant in J/K. mol and T is temperature. The value of 55.5 in the above equation is the concentration of water in the solution in mol/liter. The equilibrium constant (K) has been replaced by the equation K. By plotting (log K) against (1/T) the value of ΔG_{ads} can be calculated (ΔG_{ads} =−2.303 *R * Slope) from the slope of the straight line obtained

Generally, values of $\Delta G°_{ads} \leq$ −20 kJ/ mol signify physisorption, and values more negative than −40 kJ/ mol signify chemisorption. The negative values of ΔG_{ads} show the strong interaction and spontaneous adsorption of the inhibitor molecules onto the mild steel surface [29].

The values of $-\Delta G_{ads}$ up to 20 kJ/ mol or less than 20 kJ /mol imply the Coulombic electrostatic interactions exist between the charged molecules and the charged metal surface [30]. The values greater than 40 kJ/ mol imply the formation of the chemical bond between the inhibitor molecule and the metal surface through charge sharing or charge transfer [31].

However, adsorption is a separation process involving two phases between which certain components can be described by two main types of interaction, i.e., physical as well as chemical adsorption. The higher values of K_{ads} refer to higher adsorption and a higher inhibiting effect of inhibitors [30].

Table 6: Adsorption quantities obtained by Temkin isotherm

Condition	Temp., K	Surface coverage (θ)	Equilibrium constant of adsorption, K_{ads}	ΔG_{ads}, KJ/mol.
50 ppm of (5) with 0.3 N HCl	308	0.2114	2144.56	89.34056
	318	0.3310	3958.146	
	328	0.6291	13569.16	
	338	0.8491	45015.24	

REFERENCES
1. Elkadi L, Mernari B, Traisnel M, Bentiss F and Lagrenee M. The inhibition action of 3,6-bis(2-methoxyphenyl)-1,2-dihydro-1,2,4,5-tetrazine on the corrosion of mild steel in acidic media. Corros Sci. 2000;42(4):703-719.
2. Zhang S, Tao Z, Liao S and Wu F. Substitutional adsorption isotherms and corrosion inhibitive properties of some oxadiazol-triazole derivative in acidic solution. Corros Sci. 2010; 52(9):3126-3132.
3. Bentiss F, Traisnel M, Gengembre L and Lagrenée M. Inhibition of acidic corrosion of mild steel by 3,5-diphenyl-4H-1,2,4-triazole. Appl Surf Sci. 2000;161(1-2):194-202.
4. Al-Azzawi A and Hammud K. Inhibitive heteroamic acid behavior against 0.3N sulfuric acid co
5. rrosion of carbon steel. J. Chem Pharmaceu. Res. 2014;6(7):2808-2819.
6. Gece G. Drugs: A review of promising novel corrosion inhibitors. Corros Sci. 2011; 53(12): 3873-3898.

7. Salimon J, Salih N, Hameed A, Ibraheem H and Yousif E. Synthesis and Antibacterial Activity of Some New 1,3,4-Oxadiazole and 1,3,4-Thiadiazole Derivatives. J Appl Sci Res. 2010; 6(7):866-870.

8. Husain A and Ajmal M. Synthesis of novel 1,3,4-oxadiazole derivatives and their biological properties. Acta Pharma. 2009;59:223-233.

9. Nazim S, Farooqui M and Durrani A. Synthesis of some novel 1,3,4-oxadiazole. World J Pharmacy Pharmaceu Sci. 2014;3(5):742-748.

10. Abu-Orabi S, Abu-Naaja N and Al-Momani L. Synthesis, Study and Characterization of some 1,2,3-Triazolo-1,3,4- Oxadiazole Derivatives via Dehydration Reactions of Carbohydrazides. Jordan J Chem. 2010; 5(4): 325-330; Zaafarany I. Phenyl Phthalimide as Corrosion Inhibitor for Corrosion of C-Steel in Sulphuric Acid Solution. Portugaliae Electrochimica Acta. 2009; 27(5):631-643.

11. Al-Obaidi K. Science of imide with study case in Iraq: A mini review. Der Chemica Sinica 2015; 6(7):14-21.

12. Al-Obaidi K. Synthesis, characterization of new heterocyclic derivatives, and studying the possibility for their applications as surfactants, antimicrobial agents and corrosion inhibitors, Department of Chemistry, College of Science, Baghdad University, Baghdad, Iraq, 2013.

13. Hijji Y and E. Benjamin E. Efficient microwave assisted syntheses of unsubstituted cyclic imides. Heterocycles 2006;68:2259-2267.

14. Vogel A. Vogel 's A Textbook of Practical Organic Chemistry, 5th (Ed.), revised by B. Furniss, A. Hannaford, P. Smith, and A. Tatchell, Longman group limited, London, UK, 1989.

15. Saha A, Kumar R, Kumar R and Devakumar C. Development and assessment of green synthesis of hydrazides. Indian J Chem. 2010;49B(04):526-531.

16. Moldovan C, Oniga, A. Pârvu, B. Tiperciuc B, Verite P, Pîrnau A, Crisane O, Bojit M and Pop R. Synthesis and anti-inflammatory evaluation of some new acyl-hydrazones bearing 2-aryl-thiazole. Eur J Med Chem. 2011;46(2):526-534.

17. Chavan A and Pai N. Synthesis and Biological Activity of N-Substituted-3-chloro-2-azetidinones. Molecules 2007;12(11):2467-2477.

18. Bockris J and Reddy A. Modern Electrochemistry, Ionics, Vol. 2, 2nd (Ed.), Kluwer Academic Publishers, New York, USA, 2002.

19. El- Sayed A. Phenothiazine as inhibitor of the corrosion of cadmium in acidic solutions. J. Appl. Electrochem. 1997; 27(2): 193-200; Poornima T, Jagannatha N, and Shetty A. Studies on Corrosion of Annealed and Aged 18 Ni 250 Grade Maraging Steel in Sulphuric Acid Medium Portugaliae Electrochimica Acta. 2010;28(3):173-188.

20. Fontana M and Greene N. Corrosion Engineering, 3rd (Ed.), McGraw-Hill, New York, USA, 1987.

21. Ahmed Z. Principles of Corrosion engineering and Corrosion Control, Elsevier Science & Technology Books, New York, USA. 2006.

22. Popova A, Sokolova E, Raicheva S and Chritov M. AC and DC study of the temperature effect on mild steel corrosion in acid media in the presence of benzimidazole derivatives. Corros. Sci. 2003;45(1):33-58.

23. Morad M and Kamal El-Dean A. 2,2′-Dithiobis(3-cyano-4,6-dimethylpyridine): A new class of acid corrosion inhibitors for mild steel. Corros Sci. 2006;48(11):3398-3412; Behpour M, Ghoreishi S, Soltani N, Salavati-Niasari M, Hamadanian M, and Gandomi A. Electrochemical and theoretical investigation on the corrosion inhibition of mild steel by thiosalicylaldehyde derivatives in hydrochloric acid solution. Corros Sci. 2008;50(8):2172-2181.

24. Tang L, Li X, Li L, Mu G and Liu G. The effect of 1-(2-pyridylazo)-2-naphthol on the corrosion of cold rolled steel in acid media: Part 2: Inhibitive action in 0.5 M sulfuric acid. Mater. Chem. Phys. 2006;97:301.

25. Badawi A, Hegazy M, El-Sawy A, Ahmed H, and Kamel W. Novel quaternary ammonium hydroxide cationic surfactants as corrosion inhibitors for carbon steel and as biocides for sulfate reducing bacteria (SRB). Mater Chem Phys. 2010;124:458-465.

26. Yadav D and Quraishi M. Application of Some Condensed Uracils as Corrosion Inhibitors for Mild Steel: Gravimetric, Electrochemical, Surface

Morphological, UV–Visible, and Theoretical Investigations. Ind. Eng. Chem Res. 2012;51(46):14966-14979.

27. Ahamad I, Prasad R and Quraishi M. Experimental and theoretical investigations of adsorption of fexofenadine at mild steel/hydrochloric acid interface as corrosion inhibitor. J Solid State Electrochem. 2010;14:2095-2105.

28. Baek S, Kim Y, Yoo S, Chung K, Kim N and Kim J. Synthesis and Rust Preventing Properties of Dodecyl Succinate Derivatives Containing Triazole Groups. Ind Eng Chem Res. 2012;51: 9669-9678.

29. Fekry A and Mohamed R. Acetyl thiourea chitosan as an eco-friendly inhibitor for mild steel in sulphuric acid medium. Electrochimica Acta 2010;55(6):1933-1939.

30. Quraishi M, Rawat J and Ajmal M. Dithiobiurets: a novel class of acid corrosion inhibitors for mild steel. J Appl Electrochem. 2000;30(6):745-751.

31. Saliyan V and Adhikari A. Quinolin-5-ylmethylene-3-{[8-(trifluoromethyl)quinolin-4-yl]thio}propanohydrazide as an effective inhibitor of mild steel corrosion in HCl solution. Corros Sci. 2008;50(1):55-61.